

Design and synthesis of solution processable small molecules towards high photovoltaic performance

Zaifang Li, Qingfeng Dong, Yaowen Li, Bin Xu, Meng Deng, Jianing Pei, Jibo Zhang, Feipeng Chen, Shanpeng Wen, Yajun Gao and Wenjing Tian*

Received 3rd August 2010, Accepted 26th October 2010

DOI: 10.1039/c0jm02510k

We successfully synthesized a series of novel symmetrical solution processable small molecules (APPM, AAPM and ATPM) consisting of the electron-accepting moiety (2-pyran-4-ylidenemalononitrile) (PM) and the electron-donating moiety (triphenylamine) linked by different electron-donating moieties (phenothiazine, triphenylamine and thiophene) through a Suzuki coupling reaction. Differential scanning calorimetry (DSC) measurement indicates that APPM and AAPM shows relatively high glass-transition temperature of *ca.* 137 °C and 163 °C, while the melting point of ATPM is at *ca.* 164 °C. UV-vis absorption spectra show that the combination of the PM moiety with moieties with a gradually increased electron-donating ability results in an enhanced intramolecular charge transfer (ICT) transition, which leads to an extension of the absorption spectral range and a reduction of the band gap of the molecules. Both cyclic voltammetry measurement and theoretical calculations displayed that the highest occupied molecular orbital (HOMO) energy levels of the molecules could be fine-tuned by changing the electron-donating ability of the electron-donating moieties. The bulk heterojunction (BHJ) photovoltaic devices with a structure of ITO/PEDOT/PSS/small molecules/PCBM/LiF/Al were fabricated by using the small molecules as donors and (6,6)-phenyl C₆₁-butyric acid methyl ester (PCBM) as acceptor. Power conversion efficiencies (PCE) of 0.65%, 0.94% and 1.31% were achieved for the photovoltaic devices based on APPM/PCBM, AAPM/PCBM and ATPM/PCBM under simulated AM 1.5 illumination (100 mW cm⁻²), respectively. The open circuit voltage of 1.0 V obtained from the device based on ATPM/PCBM is one of the highest values for organic solar cells based on solution processable small molecules.

Introduction

Photovoltaic devices based on organic semiconductors are evolving into a promising cost-effective alternative to silicon-based solar cells due to their low-cost fabrication through solution processing, lightweight nature, as well as excellent compatibility with flexible substrates.^{1,2} To date, the highest power conversion efficiency (PCE) of the bulk heterojunction (BHJ) polymer photovoltaic devices has been up to 7.73%.³ Generally, polymers have many advantages: such as strong absorption ability, admirable solution processability, good film-forming ability and tunable energy levels. However, the purification of polymers is still one of the most difficult problems troubling people. And as usual, a polymer is a mixture of molecules with different molecular weight. The impurity and relatively high molecular weight dispersity would significantly decrease the charge carrier mobility of polymers and further lead

to a relatively low fill factor (FF) and PCE of the photovoltaic devices.^{4,5}

In contrast with polymers, small molecules have attracted more and more attention for photovoltaic applications due to their high purity, high charge carrier mobility (15 cm² V⁻¹ s),⁶ solution processability, well-defined molecular structures and definite molecular weights. Until now, profound progress has been achieved in the synthesis of new solution processable small molecules and the corresponding photovoltaic applications.⁷⁻¹⁶ Although the highest PCE of a solution processable bulk-heterojunction photovoltaic device based on small molecules has reached 4.4%,¹⁶ the mismatch between the absorption spectrum of small molecules and the solar spectrum is still one of the primary problems for improving the PCE of photovoltaic devices.

Recently, people have paid more and more attention to the design and synthesis of small molecules with donor-acceptor (D-A) structure.^{7,8,14-17} The intramolecular charge transfer (ICT) from the donor moiety to the acceptor moiety inside a D-A molecule can efficiently extend the absorption spectrum of the molecule for better matching the solar spectrum. Moreover, the

Jilin University - State Key Laboratory of Supramolecular Structure and Materials, Changchun, 130012, China

incorporation of functional moieties with varied electron-donating ability will bring different degrees of ICT to the conjugated system and thus provide a means to tune the optical band gap, electrochemical properties and energy levels for achieving low band gap, good air stability and high open circuit voltage (V_{oc}) small molecules.¹⁸ There are two requests for the energy level of the D–A small molecules for achieving high performance. One is the LUMO energy level of the donor must be higher than that of the electron acceptor (at least 0.3 eV) so as to drive the electron transfer from the donor to the acceptor sufficiently. The other is the HOMO energy level of the donor molecule must be low enough in order to get relatively high V_{oc} which is determined by the difference between the HOMO energy level of the donor and the LUMO energy level of the acceptor.¹⁹

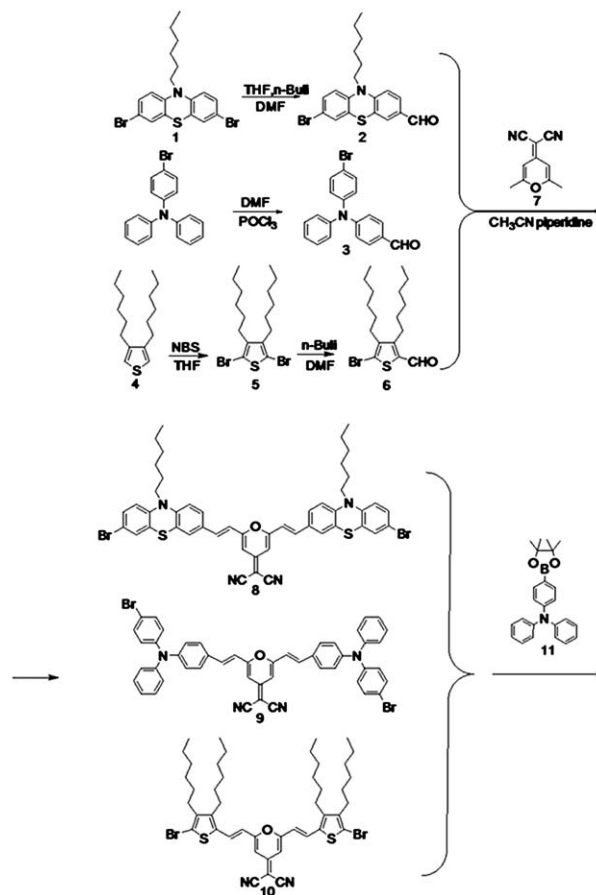
In recent years, a series of D–A small molecules based on triphenylamine (TPA) had been synthesized and applied to photovoltaic devices.^{20–22} These small molecules possessed good film-forming ability, excellent solubility and the relatively high V_{oc} . However, these small molecules exhibited relatively narrow absorption range from 300 to 630 nm, and the total photon energy among this range is rather small considering the whole solar spectra. For example, the D–A small molecules TPA-BT (with benzothiadiazole as the acceptor, TPA as the donor) and B(TPA-BT-HT) (with benzothiadiazole as the acceptor, TPA and thiophene as the donor) showed relatively narrow absorption bands from 300 to 600 nm for TPA-BT and 300 to 630 nm for B(TPA-BT-HT)^{20,22} which could be caused by the relatively weak electron-withdrawing abilities of benzothiadiazole resulting in the relatively weak ICT intensity from the electron-donating moiety (TPA, TPA and thiophene) to electron-accepting moiety (benzothiadiazole) and thus the narrow absorption range. We previously reported three D–A small molecules²¹ with sulfonyldibenzene as the acceptor and different numbers of triphenylamines as donors. The molecules exhibited good film-forming abilities, but the absorption range only covered 300 to 550 nm due to the relatively weak electron-withdrawing abilities of sulfonyldibenzene.

Herein, a series of novel symmetrical solution processable small molecules (APPM, AAPM and ATPM) consisting of the electron-donating moiety (triphenylamine) and the electron-accepting moiety (2-pyran-4-ylidenemalononitrile) (PM) linked by different electron-donating moieties (phenothiazine, triphenylamine and thiophene) were designed and synthesized towards wider absorption spectra. In these small molecules, TPA was introduced as the end group for its typical electron-donating ability, excellent hydrotropy and good film-forming ability.^{23–25} PM was introduced because of its stronger electron-withdrawing abilities than reported for the electron-accepting moiety (such as benzenamine and sulfonyldibenzene), which could enhance the ICT intensity and thus broaden the absorption spectra when combined with strong electron-donating moieties.^{7,8,18} The purpose of incorporating different electron-donating ability moieties (phenothiazine, triphenylamine and thiophene) is to further strengthen the conjugated degrees and thus the ICT intensity. Furthermore, the incorporation of different electron-donating ability moieties (phenothiazine, triphenylamine and thiophene) could regulate the oxidation potential of these small molecules and thus provide a method for tuning the energy level of the conjugated system. UV-vis absorption spectra illustrated

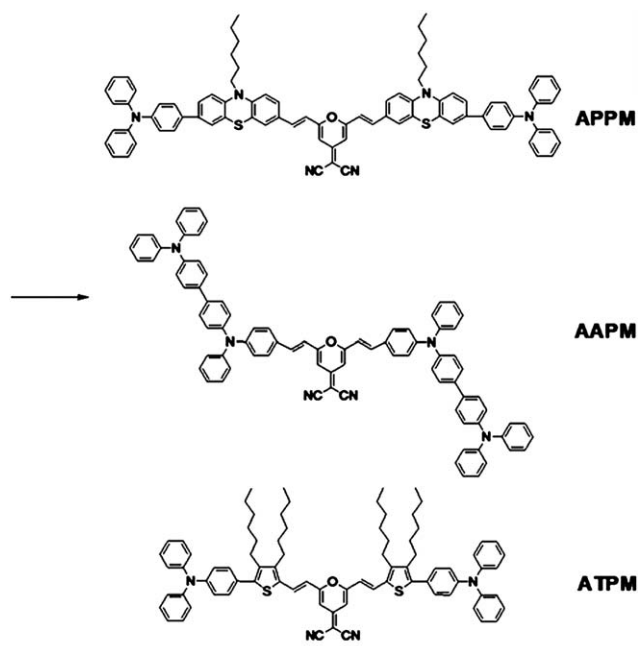
that the combination of PM moiety and TPA moiety linked by phenothiazine, triphenylamine and thiophene moieties results in an enhanced intramolecular charge transfer (ICT) transition, which lead to an extension of the absorption spectral range (*ca.* 350 nm to 700 nm). Cyclic voltammetry measurement displayed that the HOMO energy levels were fine-tuned (5.04 eV, 5.12 eV and 5.25 eV) by introducing different electron-donating moieties (phenothiazine, triphenylamine and thiophene) into these small molecules. The bulk heterojunction photovoltaic devices were fabricated by using small molecules (APPM, AAPM and ATPM) as the donor and PCBM as the acceptor. The optimized photovoltaic devices exhibited that the gradually increased PCE (0.65% for APPM, 0.94% for AAPM and 1.31% for ATPM) was achieved because of the gradual increase of V_{oc} (0.8 V for APPM, 0.9 V for AAPM and 1.0 V for ATPM) and short-circuit current (2.33 mA cm⁻² for APPM, 2.89 mA cm⁻² for AAPM and 3.85 mA cm⁻² for ATPM) under simulated AM 1.5 illumination (100 mW cm⁻²).

Experimental

All reagents and chemicals were purchased from commercial sources (Aldrich, Across, Fluka) and used without further purification unless stated otherwise. All solvents were distilled over appropriate drying agent(s) prior to use and were purged with nitrogen. Compounds **1**, **4**, **7** and **11** were synthesized



Scheme 1 Synthetic routes for compounds.



Scheme 2 Synthetic routes and structures of small molecules.

according to the literature procedure.^{18,27–29} The synthesis routes are shown in Scheme 1 while the molecular structures (APPM, AAPM and ATPM) are shown in Scheme 2.

Synthesis of compound 2

N-BuLi (6.86 mL of 2.5 M solution in hexane, 17.08 mmol) was added dropwise to a solution of compound **1** (7.56 g, 17.08 mmol) in THF (150 mL) at -78°C under a dry argon atmosphere. The solution was stirred at -78°C for 2 h, then dried DMF (1.45 mL, 18.90 mmol) was added quickly and it was kept at room temperature and stirred for 24 h before being poured into water. The product was extracted with ether. The organic layer was subsequently washed with water and brine and dried over anhydrous magnesium sulfate (MgSO_4), and the solvent was removed by rotary evaporation. The crude product was purified by column chromatography with CH_2Cl_2 : petroleum ether (1 : 2) and yielded a yellow solid of 3.50 g (1.29 mmol, yield 53%). ^1H NMR (500 MHz, CDCl_3 , TMS): δ (ppm) 9.79 (s, 1H, $-\text{CHO}$), 7.64 (m, 1H, $-\text{Ph}$), 7.55 (m, 1H, $-\text{Ph}$), 7.23 (m, 2H, $-\text{Ph}$), 6.88 (d, 1H, $-\text{Ph}$), 6.70 (d, 1H, $-\text{Ph}$), 3.83 (t, 2H, $-\text{CH}_2$), 1.77 (m, 2H, $-\text{CH}_2$), 1.42 (m, 2H, $-\text{CH}_2$), 1.30 (m, 4H, $-\text{CH}_2$), 0.87 (m, 3H, $-\text{CH}_3$). ^{13}C NMR (75 MHz, DMSO, TMS): δ (ppm) 189.79, 150.22, 142.57, 131.22, 130.18, 130.17, 129.70, 128.34, 126.06, 124.30, 117.01, 115.72, 114.92, 48.03, 31.28, 26.55, 26.38, 22.49, 13.91.

Synthesis of compound 3

DMF (10.56 mL) was put into a 50 mL flask, kept in ice-water, and then phosphorous oxychloride (4.23 mL) was added dropwise to the stirred DMF. After 20 min, 4-bromo-*N,N*-diphenylbenzamine (5.00 g, 15.38 mmol) was added to the mixture with stirring at 60°C for 6 h. After cooling, the solution was poured into cold water. The resulting mixture was neutralized to

pH = 7 with 2 M NaOH aqueous solution and extracted with chloroform. The extract was washed with plenty of water and NaCl successively. The organic extracts were dried over anhydrous MgSO_4 , evaporated and purified with column chromatography on silica gel with ethyl acetate : petroleum ether (1 : 10) as the eluant and yielded a yellow solid of 4.59 g (13.07 mmol, yield 85%). ^1H NMR (500 MHz, CDCl_3 , TMS): δ (ppm) 9.826 (s, 1H, $-\text{CHO}$), 7.694 (d, 2H, $-\text{Ph}$), 7.435 (m, 2H, $-\text{Ph}$), 7.347 (t, 2H, $-\text{Ph}$), 7.172 (m, 3H, $-\text{Ph}$), 7.035 (m, 4H, $-\text{Ph}$). ^{13}C NMR (75 MHz, DMSO, TMS): δ (ppm) 190.388, 132.718, 132.063, 131.280, 129.827, 129.281, 127.130, 126.211, 125.173, 124.408, 123.944, 123.271, 119.869.

Synthesis of compound 5

To a solution of **1** (5.5 g, 20 mmol) in THF (30 mL) at room temperature was added *N*-bromosuccinimide (7.2 g, 40 mmol) over a period of 5 min. The solution was stirred at room temperature for 4 h. The solvent was then removed *in vacuo* and hexane (200 mL) was added (to precipitate all the succinimide). The mixture was filtered through a silica plug (to remove the succinimide) and the solvent was removed *in vacuo*. Distillation under vacuum yielded a colorless oil of 6.73 g (16.4 mmol, yield 82%). ^1H NMR (500 MHz, CDCl_3 , TMS): δ (ppm) 2.560 (t, 4H, $J = 8.0$ Hz, $-\text{CH}_2$), 1.517 (m, 4H, $-\text{CH}_2$), 1.442–1.353 (m, 12H, $-\text{CH}_2$), 0.948 (t, 6H, $J = 8.0$ Hz, $-\text{CH}_3$).

Synthesis of compound 6

The synthetic procedure for compound **6** was similar to that for compound **2** and yielded a red brown oil of 0.46 g (1.29 mmol, yield 53%). ^1H NMR (500 MHz, CDCl_3 , TMS): δ (ppm) 9.912 (s, 1H, $-\text{CHO}$), 2.872 (t, 2H, $-\text{CH}_2$), 2.542 (t, 2H, $-\text{CH}_2$), 1.573 (m, 2H, $-\text{CH}_2$), 1.495 (m, 2H, $-\text{CH}_2$), 1.397 (m, 4H, $-\text{CH}_2$), 1.322 (m, 8H, $-\text{CH}_2$), 0.899 (m, 6H, $-\text{CH}_3$). ^{13}C NMR (75 MHz, CDCl_3 , TMS): δ (ppm) 181.231, 151.359, 143.693, 138.249, 122.477, 32.227, 31.459, 31.429, 29.364, 29.214, 27.908, 27.714, 22.528, 22.483, 13.989.

Synthesis of compound 8

A mixture of compound **2** (3.41 g, 8.73 mmol), compound **7** (0.69 g, 3.97 mmol), piperidine (10 drops), and acetonitrile (30 mL) were refluxed under N_2 for 24 h. The reaction mixture was cooled to room temperature and poured into water and extracted with chloroform. The combined organic extractions were washed three times with water, dried over anhydrous MgSO_4 , evaporated under vacuum and purified with column chromatography on silica gel with dichloromethane : petroleum ether (3 : 1) as the eluant to yield a red solid of 2.92 g (3.19 mmol, yield 73.5%). ^1H NMR (500 MHz, CDCl_3 , TMS): δ (ppm) 7.351 (m, 4H, $-\text{Ph}$, $-\text{vinylic}$), 7.302 (m, 2H, $-\text{Ph}$), 7.255 (m, 4H, $-\text{Ph}$), 6.862 (4d, H, $-\text{Ph}$), 6.721 (d, 2H, $-\text{Ph}$), 6.623 (s, 2H, $-\text{PM}$), 6.591 (d, $J = 16$ Hz, 2H, $-\text{vinylic}$), 3.844 (t, 4H, $-\text{CH}_2$), 1.801 (m, 4H, $-\text{CH}_2$), 1.442 (m, 4H, $-\text{CH}_2$), 1.319 (m, 8H, $-\text{CH}_2$), 0.892 (t, 6H, $-\text{CH}_3$). ^{13}C NMR (75 MHz, CDCl_3 , TMS): δ (ppm) 158.221, 155.588, 146.731, 143.133, 136.352, 130.204, 129.682, 129.101, 127.722, 126.404, 125.962, 124.571, 116.845, 116.503, 115.501, 115.426, 115.118, 106.704, 59.032, 47.901, 31.384, 26.662, 26.501, 22.575, 13.982.

Synthesis of compound 9

The synthetic procedure for compound **9** was similar to that for compound **8** and yielded a red solid of 2.02 g (2.40 mmol, 83.1%). ¹H NMR (300 MHz, CDCl₃, TMS): δ (ppm) 7.405 (m, 10H, -Ph), 7.323 (m, 4H, -Ph, -vinylic), 7.140 (t, 6H, -Ph), 7.026 (m, 8H, -Ph), 6.643 (s, 2H, -PM), 6.614 (d, 2H, *J* = 16.2 Hz, -vinylic), ¹³C NMR (75 MHz, CDCl₃, TMS): δ (ppm) 158.589, 156.741, 149.432, 146.296, 145.866, 137.243, 132.529, 129.666, 129.048, 128.025, 126.538, 125.554, 124.633, 121.976, 116.632, 116.099, 115.518, 106.433, 58.540.

Synthesis of compound 10

The synthetic procedure for compound **10** was similar to that for compound **8** and yielded a dark green solid of 2.1 g (2.46 mmol, 53.2%). ¹H NMR (500 MHz, CDCl₃, TMS): δ (ppm) 7.509 (d, 2H, *J* = 15.5 Hz, -vinylic), 6.613 (s, 2H, -PM), 6.368 (d, 2H, *J* = 15.5 Hz, -vinylic), 2.678 (t, 4H, -CH₂), 2.529 (t, 4H, -CH₂), 1.500 (m, 8H, -CH₂), 1.332 (m, 16H, -CH₂), 1.285 (m, 8H, -CH₃), 0.908 (t, 6H, -CH₃), 0.843 (t, 6H, -CH₃). ¹³C NMR (75 MHz, CDCl₃, TMS): δ (ppm) 157.792, 157.693, 155.164, 144.954, 143.322, 134.634, 127.844, 116.501, 115.133, 113.724, 106.635, 59.598, 31.445, 31.420, 29.343, 29.191, 28.312, 27.960, 22.486, 13.951, 13.868.

General procedures of small molecules

Suzuki coupling reaction was used to synthesize small molecules shown in Scheme 1 and Scheme 2. compound **8**, (or **9** or **10**), compound 11, and (PPh₃)₄Pd(0) (2 mol% with respect to compound **8** or **9** or **10**) were dissolved in a mixture of toluene (6 mL) and aqueous 2 M K₂CO₃ (4 mL, 3/2 volume ratio). The solution was stirred under the Ar atmosphere and refluxed with vigorous stirring for 48 h. The resulting solution was then poured into water and was extracted with dichloromethane. The extract was washed with brine and dried over anhydrous MgSO₄.

Synthesis of compound APPM

After evaporation of the solvent, the residue was purified with column chromatography on silica gel with dichloromethane : petroleum ether (2 : 1) as the eluant to dark red solid 473 mg (0.38 mmol, 76.0%). ¹H NMR (500 MHz, CDCl₃, TMS): δ (ppm) 7.354 (m, 14H, -Ph), 7.273 (d, 2H, -Ph), 7.250 (s, 2H, -Ph), 7.116 (t, 12H, -Ph), 7.031 (t, 4H, -Ph), 6.875 (d, 4H, -Ph), 6.591 (d, 4H, -PM, -vinylic), 3.887 (m, 4H, -CH₂), 1.844 (m, 4H, -CH₂), 1.471 (m, 4H, -CH₂), 1.339 (m, 8H, -CH₂), 0.894 (m, 6H, -CH₃). ¹³C NMR (75 MHz, CDCl₃, TMS): δ (ppm) 158.293, 155.554, 147.611, 147.083, 146.830, 142.467, 136.455, 135.004, 133.497, 129.250, 128.883, 128.739, 127.852, 127.086, 126.238, 125.547, 125.225, 124.743, 124.382, 123.887, 122.945, 116.088, 115.784, 115.484, 115.140, 106.480, 58.731, 47.881, 31.387, 26.743, 26.541, 22.580, 13.951. MALDI-TOF MS: calcd for C₈₄H₇₂N₆OS₂ 1245.64; found 1245.60.

Synthesis of compound AAPM

After evaporation of the solvent, the residue was purified with column chromatography on silica gel with dichloromethane : petroleum ether (1 : 1) as the eluant to dark red solid

468 mg (0.40 mmol, 80.0%). ¹H NMR (500 MHz, CDCl₃, TMS): δ (ppm) 7.522 (d, 4H, -Ph), 7.455 (m, 10H, -Ph), 7.345 (t, 4H, -Ph), 7.283 (t, 4H, -Ph), 7.200 (m, 8H, -Ph), 7.153 (t, 13H, -Ph), 7.102 (d, 4H, -Ph), 7.049 (t, 4H, -Ph), 6.651 (s, 2H, -PM), 6.623 (d, 2H, -vinylic). ¹³C NMR (75 MHz, CDCl₃, TMS): δ (ppm) 158.731, 155.830, 149.894, 147.636, 147.096, 146.627, 145.486, 137.431, 136.425, 134.205, 129.607, 129.274, 129.037, 127.582, 127.382, 125.610, 125.529, 124.422, 124.388, 124.378, 123.882, 122.988, 121.745, 115.780, 115.854, 106.340, 58.270. MALDI-TOF MS: calcd for C₈₄H₆₀N₆O 1169.41; found 1169.50.

Synthesis of compound ATPM

After evaporation of the solvent, the residue was purified with column chromatography on silica gel with dichloromethane : petroleum ether (2 : 3) as the eluant to dark red solid 426 mg (0.36 mmol, 72.0%). ¹H NMR (300 MHz, CDCl₃, TMS): δ (ppm) 7.033 (d, 2H, *J* = 15.6 Hz, -vinylic), 7.297 (d, 8H, -PH), 7.248 (s, 4H, -PH), 7.146 (d, 8H, -PH), 7.068 (t, 8H, -PH), 6.581 (s, 2H, -PM), 6.447 (d, 2H, *J* = 15.6 Hz, -vinylic), 2.719 (t, 4H, -CH₂), 2.586 (t, 4H, -CH₂), 1.421 (m, 32H, -CH₂), 0.853 (t, 12H, -CH₃). ¹³C NMR (75 MHz, CDCl₃, TMS): δ (ppm) 158.328, 155.438, 147.887, 147.319, 146.953, 141.858, 139.406, 132.873, 129.780, 129.374, 128.816, 127.538, 124.929, 123.474, 122.529, 115.672, 115.618, 106.249, 58.353, 31.840, 31.615, 31.388, 30.721, 29.489, 29.348, 27.830, 27.314, 22.614, 22.522, 14.002, 13.945. MALDI-TOF MS: calcd for C₈₀H₈₆N₄OS₂ 1245.64; found 1245.60.

Instruments and measurements

Differential scanning calorimetry (DSC) was performed under nitrogen flushing at a heating rate of 20 °C min⁻¹ with a NETZSCH (DSC-204) instrument. ¹H NMR and ¹³C NMR spectra were measured using a Bruker AVANCE-500 NMR spectrometer spectrometer and a Varian Mercury-300 NMR, respectively. The time-of-flight mass spectra were recorded with a Kratos MALDI-TOF mass system. UV-visible absorption spectra were measured using a Shimadzu UV-3100 spectrophotometer. The photoluminescence spectra of spin-cast films and solution were measured with a RF-5301PC spectrofluorophotometer. Electrochemical measurements of these derivatives were performed with a Bioanalytical Systems BAS 100 B/W electrochemical workstation. Atomic force microscopy (AFM) images of blend films were carried out using a Nanoscope IIIa Dimension 3100.

Fabrication and characterization of photovoltaic devices

For device fabrication, the ITO glass was precleaned and modified by a thin layer of PEDOT/PSS, which was spin-cast from a PEDOT:PSS aqueous solution (H. C. Starck) on the ITO substrate, and the thickness of the PEDOT/PSS layer was about 50 nm. The active layer contained a blend of small molecules as electron donor and PCBM as electron acceptor, which was prepared from chloroform and chlorobenzene solution with the different weight ratios (small molecule : PCBM = 2 : 1, 1 : 1, 1 : 2, and 1 : 3, respectively). After spin-coating the blend from solution at 900 rpm, The devices were completed by evaporating a 0.6 nm LiF layer and protected by 100 nm of Al at a base

pressure of 5×10^{-4} Pa. The effective photovoltaic area as defined by the geometrical overlap between the bottom ITO electrode and the top cathode was 5 mm^2 . The current–voltage (*J–V*) characteristics were recorded using Keithley 2400 Source Meter in the dark and under simulated AM 1.5 illumination (100 mW cm^{-2}) by Solar Simulators (SCIENCETECH SS-0.5 K). The spectral response was recorded by SR830 lock-in amplifier under short circuit condition when devices were illuminated with a monochromatic light from a Xenon lamp. Films thickness was measured by Veeco DEKTAK 150 surface profilometer. AFM images were measured by atomic force microscopy (S II Nano-navi probe station 300hv). All fabrication and characterizations were performed in an ambient environment.

Material synthesis and structural characterization

The general synthetic routes toward the compounds and the final small molecules are outlined in Scheme 1. The compounds **8**, **9** and **10** were prepared through Knoevenagel condensation of compound **7** with **2**, **3** and **6** respectively. The structures of compounds were confirmed by ^1H NMR, ^{13}C NMR spectra, and the data were included in the Experimental section. In ^1H -NMR spectroscopy of compound **8**, **9** and **10**, the coupling constant ($J \sim 15.5 \text{ Hz}$) of olefinic protons indicates that the Knoevenagel reaction afforded the pure all-*trans* isomers. The final products (shown in Scheme 2) were prepared by the well-known palladium-catalyzed Suzuki coupling reaction between varied compounds (**8**, **9**, **10**) and compound **11**. ^1H NMR and ^{13}C NMR spectras were used to characterize the structure of these molecules, which clearly indicate that well-defined APPM, AAPM and ATPM have been obtained. The two legible double peaks that appear at $\sim 6.400 \text{ ppm}$ and 7.600 ppm with the coupling constant ($J \sim 16 \text{ Hz}$) are due to all-*trans* double bond, which further confirms the regular structure. Molecular weights were determined by Kratos MALDI-TOF. These results are consistent with the proposed structure and molecule weights. All the molecules exhibited excellent solubility in common organic solvents such as chloroform, tetrahydrofuran, dichloromethane, and chlorobenzene.

Thermal properties

Differential scanning calorimetry (DSC) was performed to investigate the thermal properties of APPM, AAPM and ATPM. Fig. 1 shows the DSC curves of these molecules after they are purified through recrystallization. When APPM and AAPM were heated, the endothermic peak due to glass transition temperatures were observed at *ca.* 137 and 163 °C respectively. When ATPM was heated, the exothermic peak due to crystallization was observed at *ca.* 131 °C. On further heating above the crystallization temperature, the apparently endothermic peak due to melting point was observed at *ca.* 164 °C.

Optical properties

The normalized UV-vis absorption spectra of APPM, AAPM and ATPM in dilute chloroform solution (concentration 10^{-5} M) are shown in Fig. 2a, and the main optical properties are listed in Table 1. ATPM with the weak electron-donating moiety (thiophene) showed three absorption peaks at 312 nm, 400 nm and

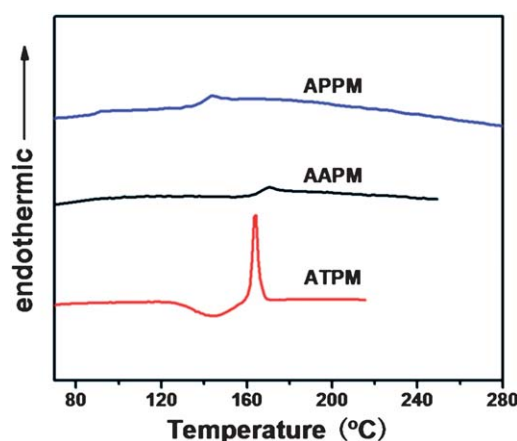


Fig. 1 Differential scanning calorimetry (DSC) measurement of APPM, AAPM and ATPM, scan rate $10 \text{ }^\circ\text{C min}^{-1}$.

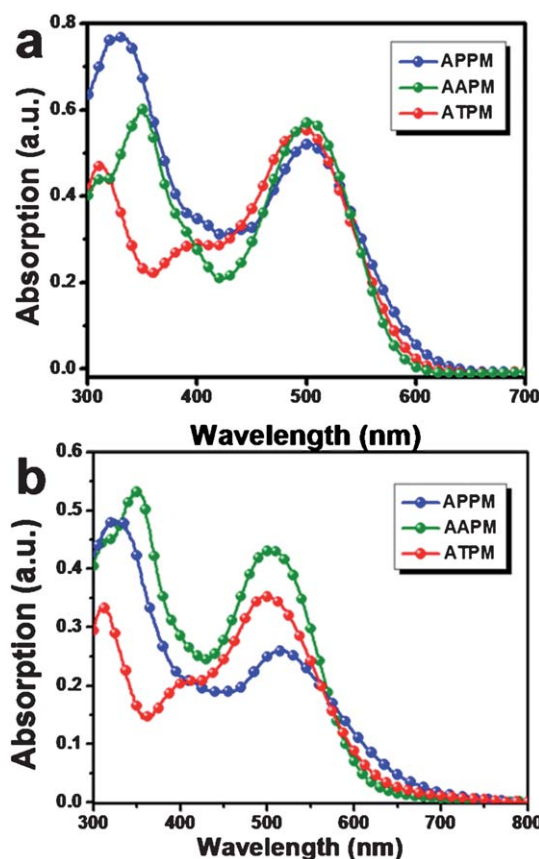


Fig. 2 The absorption spectra of the small molecules (a) in chloroform solutions with the concentration of $10^{-5} \text{ mol L}^{-1}$; (b) films spin-coated from a 10 mg mL^{-1} chloroform solution.

497 nm in dilute solution (Fig. 2a), which can be assigned to the intrinsic absorption of triphenylamine moiety, $\pi-\pi^*$ transition of the conjugated small molecule backbone and ICT interaction between the electron-donating moieties (thiophene and triphenylamine) and electron-accepting moiety (PM). The absorption spectra of APPM in dilute solutions also exhibited three absorption peaks at 328 nm, 400 nm and 503 nm corresponding to the intrinsic absorption of phenothiazine moiety, $\pi-\pi^*$

Table 1 Optical and electrochemical data of ATPM, AAPM and APPM

Small molecules	In solution ^a		In film ^b		$E_{\text{Ox}}^{\text{onset}}/V/\text{HOMO}/\text{eV}$	$E_{\text{Red}}^{\text{onset}}/V/\text{LUMO}/\text{eV}$	Electrochem. $E_{\text{g,cc}}/\text{eV}$	Optical ^c $E_{\text{g,opt}}/\text{eV}^c$
	$\lambda_{\text{max}}^{\text{abs}}/\text{nm}$ ($\epsilon_{\text{max}}/\text{M}^{-1}\text{cm}^{-1}$)	$\lambda_{\text{edge}}/\text{nm}$	$\lambda_{\text{max}}^{\text{abs}}/\text{nm}$	$\lambda_{\text{edge}}/\text{nm}$				
APPM	503 (52501)	612	512	665	0.35/−5.04	−1.21/−3.48	1.56	1.86
AAPM	502 (58496)	589	504	616	0.43/−5.12	−1.25/−3.44	1.68	2.01
ATPM	497 (56844)	603	499	638	0.56/−5.25	−1.22/−3.47	1.78	1.94

^a 1×10^{-5} M in anhydrous chloroform. ^b Spin-coated from a 10 mg mL⁻¹ chloroform solution. ^c The optical band gap ($E_{\text{g,opt}}$) was obtained from absorption edge.

transition of the conjugated small molecule backbone and ICT interaction between the electron-donating moieties (phenothiazine and triphenylamine) and electron-accepting moiety (PM), respectively. But the absorption peak from π - π^* transition of APPM becomes much weaker than that of ATPM, which could be explained by its worse conjugation as the molecular dimensions increased. In the absorption spectra of AAPM, only two absorption peaks at 350 nm and 502 nm were observed, which could be ascribed to the intrinsic absorption of triphenylamine moiety and ICT interaction between the electron-donating moieties (triphenylamine) and electron-accepting moiety (PM). The peak corresponding to π - π^* transition disappeared as molecular dimensions increased further. The solution absorption spectra of APPM, with an absorption maximum at 503 nm and the absorption edge at 612 nm, is broadened and red-shifted compared to those of ATPM (497 nm, 603 nm), and AAPM (502 nm, 589 nm), which can be explained by much stronger ICT effect in APPM than that in ATPM and AAPM. Among the three small molecules, there is a D–A–D structure, where D represents the electron-donor (thiophene, triphenylamine and phenothiazine) while A represents the electron-acceptor (2-pyran-4-ylidenemalononitrile). The stronger electron-donating ability D possesses, the higher electronic delocalization degree and the stronger ICT the molecule has. Since the order of the electron-donating abilities of the three D is phenothiazine > triphenylamine > thiophene, the strongest electron-donating ability of phenothiazine compared with triphenylamine and thiophene improves the effective conjugation length along the molecule backbone, resulting in an increase in the ICT strength and thus electronic delocalization.³⁰ Moreover, the relatively high absorption coefficients could be calculated from the Beer's law equation with the same dilute concentration of the molecules in chloroform (absorption coefficients are listed in Table 1), which assures these small molecules can absorb enough photons.

Fig. 2b shows the optical absorption spectra of the small molecules in thin films. The absorption spectra in thin films are generally similar in shape to those in dilute solution. And we could easily find that there is a little red shift of the maximum absorption peak and a certain degree of broadening for absorption edge between the absorption spectra in film and solution for the three molecules (for APPM, 9 and 53 nm; for AAPM, 2 and 27 nm; and for ATPM, 2 and 35 nm, respectively). The red shifts and broadening of absorption edge may be caused by the existence of some aggregation of the molecules, which is beneficial for π - π^* stacking in the solid state and thus could broaden their absorption spectra.³¹ As for APPM, the red shift

Table 2 Characteristic current–voltage parameters from device spin-coated from chlorobenzene solution and testing at standard AM 1.5 G conditions

Small molecule	Small molecule : PCBM	V_{oc}/v	$J_{\text{sc}}/\text{mA cm}^{-2}$	FF	PCE (%)
APPM	2 : 1	0.86	1.16	0.27	0.27
	1 : 1	0.82	1.95	0.33	0.53
	1 : 2	0.80	2.33	0.35	0.65
	1 : 3	0.78	2.20	0.35	0.60
AAPM	2 : 1	0.96	1.43	0.30	0.41
	1 : 1	0.90	1.66	0.34	0.51
	1 : 2	0.88	2.00	0.36	0.63
	1 : 3	0.90	2.89	0.36	0.94
ATPM	2 : 1	1.04	0.61	0.20	0.13
	1 : 1	1.02	2.16	0.27	0.59
	1 : 2	1.00	3.85	0.34	1.31
	1 : 3	0.92	3.50	0.36	1.16

degree of the maximum absorption peak and the broadening of absorption edge are larger than ATPM and AAPM, which maybe attributed to its smaller steric hindrance in the molecule structure than that of ATPM and AAPM. As regards AAPM, the red shift degree of the maximum absorption peak and the broadening of absorption edge is only 2 and 27 nm. This may result from its bulky steric hindrance conformations due to the existence of four triphenylamine moieties in AAPM, which is not favorable for the π - π^* stacking in the solid state. In the case of ATPM, it also exhibits only 2 nm red shift of the maximum absorption peak and 35 nm broadening of absorption edge compared with that in dilute solutions. It could be explained by the existence of triphenylamine moieties and long alkyl side chains which can increase immensely the steric hindrance in the molecule structure. As the absorption edge of the three small molecules are tuned from 616 to 665 nm, the optical band gap $E_{\text{g,opt}}$ of the three small molecules derived from the absorption edge of the thin film spectra is in the range of 2.01–1.86 eV (Table 2). As expected, APPM with the strongest intramolecular charge transfer interaction thus has the lowest optical band gap of 1.86 eV.

Electrochemical properties

Fig. 3 shows the cyclic voltammetry (CV) diagrams of the small molecules using TBAPF₆ as supporting electrolyte in methylene dichloride solution with platinum button working electrodes, a platinum wire counter electrode and an Ag/AgNO₃ reference

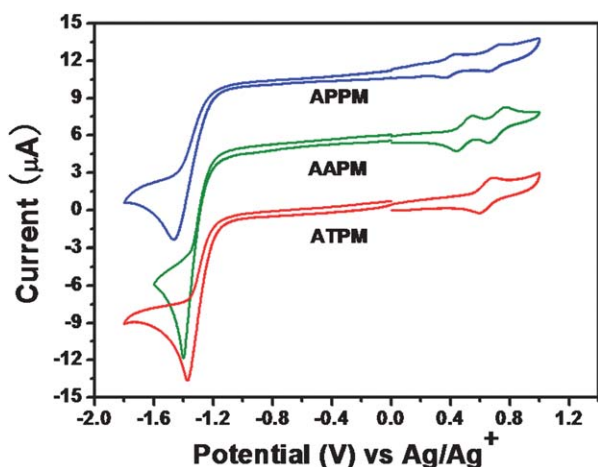


Fig. 3 Cyclic voltammograms of APPM, AAPM and ATPM solutions on platinum electrode in 0.1 mol L⁻¹ *n*-Bu₄NPF₆ in CH₂Cl₂ solution, at a scan rate of 100 mV s⁻¹.

electrode under the N₂ atmosphere. Ferrocene was used as the internal standard. The redox potential of Fc/Fc⁺ which has an absolute energy level of -4.8 eV relative to the vacuum level for calibration is located at 0.11 V in 0.1 M TBAPF₆/methylene dichloride solution.²⁶ The results of the electrochemical measurement and calculated energy levels of the small molecules are listed in Table 1.

Table 1 shows the calculated HOMO energy level (-5.04 eV) and LUMO energy level (-3.48 eV) of APPM. The LUMO energy levels of AAPM and ATPM are -3.44 and -3.47 eV, which are very similar to those of APPM and the reported PM-containing small molecules.^{7,8} Therefore, the substitution of varied electron-donating moieties with different electron-donating abilities have almost no effect on the reduction potential of the small molecules and the relatively low LUMO energy levels of the three small molecules should result from the stronger reduction of PM-based acceptor moiety.

It is clear that the HOMO levels of APPM (-5.04 eV), AAPM (-5.12 eV) and ATPM (-5.25 eV) are gradually decreased with the weakened electron-donating abilities of phenothiazine, triphenylamine and thiophene. As we know that the HOMO energy level of the small molecule is very important for high performance photovoltaic device. Firstly, the small molecule should have good air stability with HOMO energy level being below the air oxidation threshold (*ca.* -5.2 eV).³² Secondly, the open circuit potential (V_{oc}) value for the photovoltaic device is determined by the difference between the HOMO energy level of donor and LUMO energy level of acceptor, and the relatively low HOMO level of the small molecules may allow a high open circuit voltage (V_{oc}) for the photovoltaic device.³¹ Therefore, the gradually decreased HOMO levels of the small molecules are benefit for enhancing their air stability and raising their V_{oc} values.

The energy band structure of the three small molecules and PCBM is presented in Fig. 4. The first dashed line indicates the threshold for air stability, and the second dashed line represents the threshold value for an effective charge transfer from the small molecules to PCBM.^{24,33} The LUMO values of PCBM were reported to be -4.30 eV²⁴ or -4.10 eV³⁴ or around -3.70 eV.³⁵ Therefore, we measured the LUMO and HOMO values of

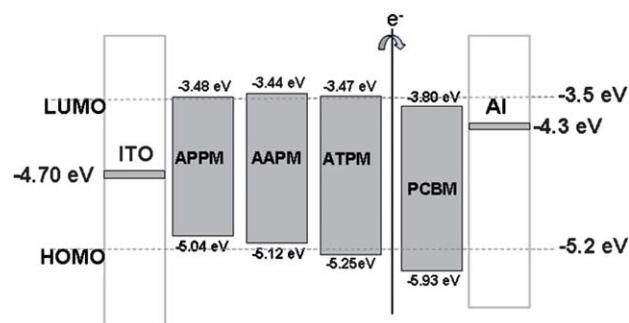


Fig. 4 Band diagram for acceptor PCBM and donors APPM, AAPM and ATPM. Dashed lines indicate the thresholds for air stability (-5.2 eV) and effective charge transfer from APPM, AAPM or ATPM to PCBM (-3.5 eV).

PCBM used in our experiments by cyclic voltammetry in the same condition as APPM, AAPM, and ATPM. The calculated values of the LUMO and HOMO energy levels of PCBM were -3.80 and -5.93 eV respectively. Therefore, the threshold value for realizing the effective charge transfer should be -3.5 eV. Furthermore, the calculated electrochemical band gaps (listed in Table 1) indicate that the relatively low band gaps were achieved (1.56 eV, 1.68 eV and 1.78 eV for APPM, AAPM and ATPM, respectively) and it is an effective manners for reducing the electrochemical band gap according to controlling the molecule structure.

Theoretical calculation

The geometry and electronic properties of APPM, AAPM and ATPM have been investigated by means of theoretical calculation with the Gaussian 03 program package at a hybrid density functional theory (DFT) level.²⁴ Becke's three-parameter gradient corrected functional (B3LYP) with a 6-31G basis was used for full geometry optimization. Fig. 5 presents the geometry, the HOMO and LUMO. H atoms were used in place of the *n*-hexyl groups to limit computation time. The calculation results demonstrate that the periplanatic PM moiety with its two adjacent phenyl vinyl moieties constitutes a large conjugated planar structure, and the triphenylamine moieties located at the end of the molecules result in a nonplanar structure for the small molecules. Electron density of the HOMO energy level

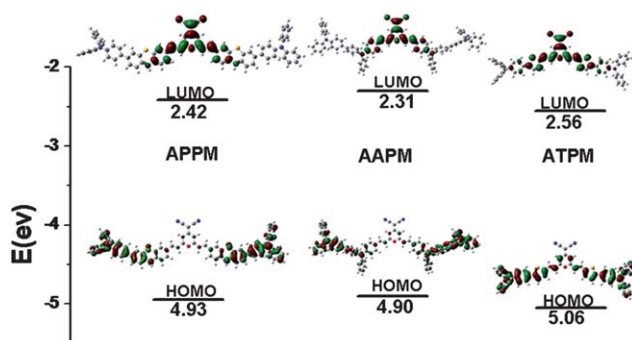


Fig. 5 Molecular orbital surfaces of the HOMO and LUMO of ATPM, AAPM, and APPM obtained at B3LYP/6-31G* level.

distributes mainly on the TPA *etc.*-donor moieties, while that of the LUMO energy level mainly delocalizes on the PM-acceptor moiety, indicating a charge-transfer nature of HOMO \rightarrow LUMO from the electron-donating moieties to the PM-acceptor moiety. Furthermore, the calculated HOMO energy levels are consistent with the electrochemical measurement while the LUMO energy levels exhibit some bias.

Photovoltaic performance

To demonstrate the application potential of the small molecules as an electron donor in organic solar cell, photovoltaic devices were fabricated by spin-coating at a constant concentration of 20 mg mL⁻¹ comprising a mixture of small molecule and PCBM. As we know that the weight ratio of donor material/PCBM have a large effect on the photovoltaic performance because there is a balance between the absorbance and the charge transporting network of the active layer in the photovoltaic devices. Too low a PCBM content will limit the electron transporting ability, while too high a PCBM content will decrease the absorbance and hole transporting ability of the active layer. Therefore, the photovoltaic devices with different weight ratios for small molecule : PCBM (2 : 1, 1 : 1, 1 : 2 and 1 : 3) were achieved using

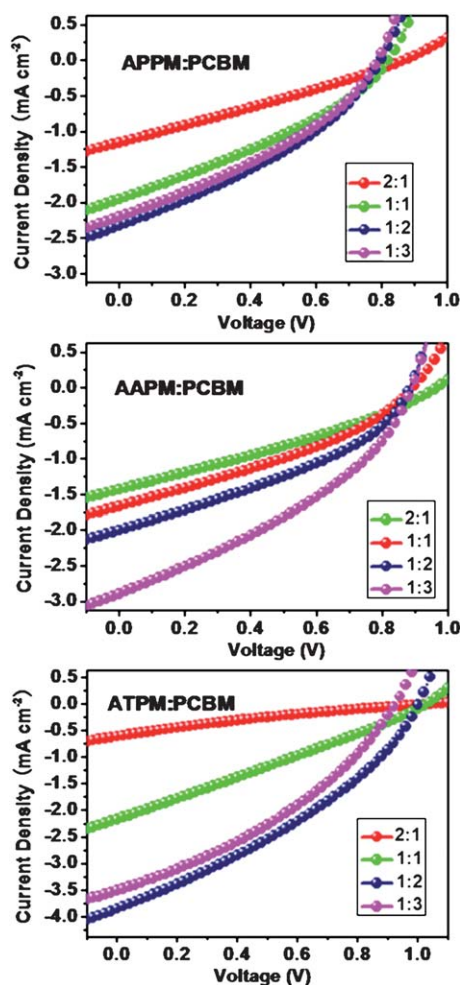


Fig. 6 Current–voltage characteristics of photovoltaic devices based on APPM, AAPM and ATPM under illumination of AM 1.5, 100 mW cm⁻².

chlorobenzene (CB) solutions. The photovoltaic parameters of the photovoltaic devices are summarized in Table 2 and the corresponding current–voltage characteristics with various blend weight ratios are presented in Fig. 6, respectively. The photovoltaic parameters of the devices are summarized in Table 2. The optimized photovoltaic devices with a structure of indium tin oxide (ITO)/PEDOT/PSS/small molecules/PCBM/LiF/Al exhibit a V_{oc} of 0.80 V, a short-circuit current (J_{sc}) of 2.33 mA cm⁻², a fill factor (FF) of 0.35, and a PCE of 0.65% for the device based on APPM/PCBM; 0.90 V, 2.89 mA cm⁻², 0.36, 0.94% for the device based on AAPM/PCBM; and 1.00 V, 3.85 mA cm⁻², 0.34, and 1.31% for the device based on ATPM/PCBM, respectively.

The optimized photovoltaic devices based on APPM, AAPM and ATPM exhibited the gradually increased V_{oc} of 0.8 V, 0.9 V and 1.0 V respectively, which is consistent with the HOMO energy level order of these small molecules (APPM > AAPM > ATPM). The result indicates that it is an effective method for achieving high V_{oc} by adjusting the electron-donating abilities of the bridge moieties (phenothiazine, triphenylamine and thiophene), and the value of 1.0 V is also one of the highest V_{oc} for photovoltaic devices.

As for J_{sc} , the higher J_{sc} of the optimized photovoltaic devices based on ATPM/PCBM (3.85 mA cm⁻²) and AAPM/PCBM (2.89 mA cm⁻²) had been obtained than that of the device based on APPM/PCBM (2.33 mA cm⁻²). This could be explained by the relatively high absorption coefficients of ATPM (56844) and AAPM (58490) than that of APPM (52501) while these molecules exhibited nearly the same absorption range. However, the J_{sc} of the device based on AAPM/PCBM is lower (2.89 mA cm⁻²) than that of ATPM (3.85 mA cm⁻²), even though AAPM possesses a higher absorption coefficient than that of ATPM.

Considering that charge carrier mobility of photovoltaic materials is another important factor which influences the J_{sc} of photovoltaic devices,³⁶ we measured the hole mobility of APPM, AAPM and ATPM by space charge limited current (SCLC) method.³⁷ The hole only devices with a structure of ITO/PEDOT/small molecule/Au were fabricated and their current–voltage

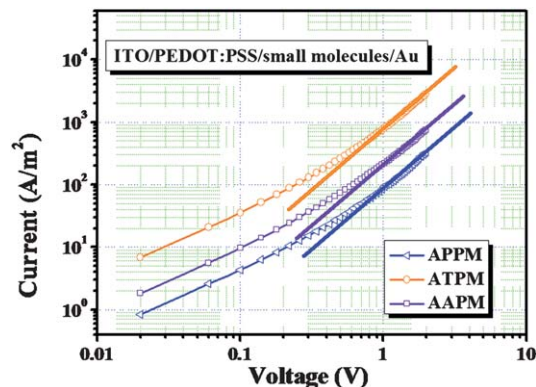


Fig. 7 J - V curve of an ITO/PEDOT/small molecule/Au device in the dark with log axis for estimating the hole mobility of APPM, AAPM, ATPM. The thicknesses of the small molecules are around 110 nm, 100 nm, 120 nm respectively. The solid line from 0.01 to 0.50 V means log J is fitted linearly dependent on log V with a slope of 1. For the solid line from 0.5 to 1.5 V log J is fitted linearly dependent on log V with a slope of 2 (SCLC area).

curves in the dark are shown in Fig. 7. The hole mobility values were measured to be $7.91 \times 10^{-6} \text{ cm}^2 \text{ v}^{-1} \text{ s}^{-1}$, $3.15 \times 10^{-5} \text{ cm}^2 \text{ v}^{-1} \text{ s}^{-1}$ and $7.47 \times 10^{-5} \text{ cm}^2 \text{ v}^{-1} \text{ s}^{-1}$ for APPM, AAPM and ATPM, respectively, which are relatively high values for donors. The gradually increased hole mobility from APPM to ATPM could be due to their enhanced conjugation.³⁶ Obviously, the hole mobility value of ATPM is higher than that of APPM and AAPM, which is well consistent with its higher J_{sc} (3.85 mA cm^{-2}) based on ATPM:PCBM than those of based on APPM:PCBM (2.89 mA cm^{-2}) and AAPM:PCBM (2.33 mA cm^{-2}). As for APPM, the lowest J_{sc} (2.33 mA cm^{-2}) might be caused by its lowest hole mobility, which leads to the charge mobility imbalance and thus could reduce the J_{sc} of the photovoltaic devices.

To gain further insight into what might affect the J_{sc} of the photovoltaic device, we analyzed the morphology of APPM/PCBM, AAPM/PCBM and ATPM/PCBM blend films. Fig. 8 shows the AFM height images of APPM/PCBM, AAPM/PCBM and ATPM/PCBM blend films with the weight ratio 1 : 2, 1 : 3 and 1 : 2, respectively. It is clearly evidenced by AFM that the APPM/PCBM and ATPM/PCBM blend films exhibit relatively flat surfaces with the root-mean-square (rms) of 0.37 nm and 0.36 nm, respectively, which demonstrate that APPM and ATPM possess the excellent film-forming abilities and

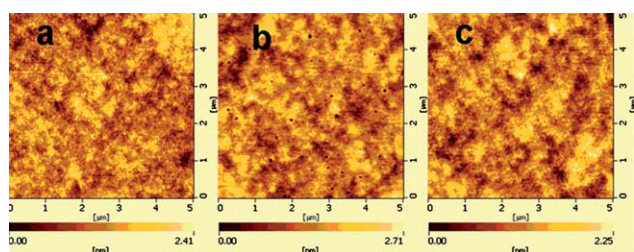


Fig. 8 Topography image (size $5 \mu\text{m} \times 5 \mu\text{m}$) obtained by tapping-mode AFM showing the morphology of the blend films spin-coated from chlorobenzene solutions for APPM, AAPM and ATPM. (a) APPM/PCBM (1 : 2 w/w); (b) AAPM/PCBM (1 : 3 w/w); (c) ATPM/PCBM (1 : 2 w/w).

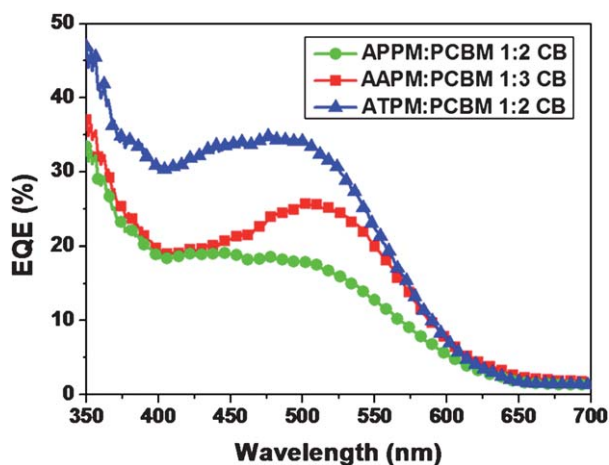


Fig. 9 External quantum efficiency (EQE) curve for device using 1 : 2, 1 : 3, 1 : 2 blend of APPM/PCBM, AAPM/PCBM, ATPM/PCBM, respectively.

miscibilities with PCBM. As for AAPM/PCBM blend film, the relatively low rms of 0.42 nm was also obtained, however, some leakage sources were observed, which indicates that AAPM possesses the worse film-forming abilities and miscibility with PCBM than APPM and ATPM. Moreover, the investigations also indicate that the lower J_{sc} (2.89 mA cm^{-2}) obtained from the AAPM/PCBM device could attribute to the existence of some leakage sources in AAPM/PCBM blend film, which is especially disadvantageous for the transport of charge carrier and thus may reduce the J_{sc} of AAPM/PCBM device.

Fig. 9 shows the external quantum efficiency (EQE) spectra of devices based on APPM/PCBM, AAPM/PCBM and ATPM/PCBM blend films with the weight ratio of 1 : 2, 1 : 3 and 1 : 2, respectively. It can be seen that all the devices show the efficient photoconversion efficiency in the range 350–650 nm, with EQE values of *ca.* 20–35%. Although the response range of these photovoltaic devices is almost equal, the maximum values are close to 18.8% at 445 nm based on APPM/PCBM, 25.4% at 506 nm based on AAPM/PCBM and 34.3% at 476 nm based on ATPM/PCBM.

The photovoltaic devices based on APPM/PCBM exhibited a PCE of 0.65%, while a PCE of 0.94% for the photovoltaic device based on AAPM/PCBM and a PCE of 1.31% for the photovoltaic device based on ATPM/PCBM under simulated AM 1.5 illumination (100 mW cm^{-2}). Compared with APPM and AAPM, ATPM based photovoltaic device exhibited higher V_{oc} , J_{sc} and thus the higher PCE while the FF stays nearly the same value. The results indicate that it is an effective way to improve PCE by adjusting the structure of small molecules and ATPM is a promising donor material for photovoltaic devices.

Conclusions

We have designed and synthesized three novel D–A conjugated small molecules consisting of electron-accepting moiety (PM) and electron-donating moiety (triphenylamine) linked by different electron-donating ability moieties (thiophene, triphenylamine and phenothiazine). Optical property investigations clearly indicated that these new small molecules exhibited long wavelength ICT absorption bands. Both the electrochemical properties and molecular orbital distribution calculations revealed that the HOMO energy levels of the resulting small molecules could be fine-tuned by changing the electron-donating ability moieties. Meanwhile, the morphologies of the blend films containing small molecules and PCBM demonstrated these small molecules possess the excellent film-forming abilities. The photovoltaic devices based on these small molecules showed the PCE in the range of 0.65–1.31%, which indicate that it is an effective way to improve the PCE of photovoltaic devices by adjusting the electron-donating abilities for the type of D–A molecules.

Acknowledgements

This work was supported by the State Key Development Program for Basic Research of China (Grant No. 2009CB623605), the National Natural Science Foundation of China (Grant No. 20874035), the 111 Project (Grant No. B06009), and the Project of Jilin Province (20080305).

References and notes

- (a) S. Gunes, H. Neugebauer and N. S. Sariciftci, *Chem. Rev.*, 2007, **107**, 1324; (b) E. Bungeard and F. C. Krebs, *Sol. Energy Mater. Sol. Cells*, 2007, **91**, 954; (c) C. J. Brabec, *Sol. Energy Mater. Sol. Cells*, 2004, **83**, 273.
- M. C. Scharber, D. Muehler, M. Koppe, P. Denk, A. Waldauf, A. J. Heeger and C. J. Brabec, *Adv. Mater.*, 2006, **18**, 789.
- H. Y. Chen, J. H. Hou, S. Q. Zhang, Y. Y. Liang, G. W. Yang, Y. Yang, L. P. Yu, Y. Wu and G. Li, *Nat. Photonics*, 2009, **3**, 649.
- R. F. Salzman, J. G. Xue, B. P. Rand, A. Alexander, M. E. Thompson and S. R. Forrest, *Org. Electron.*, 2005, **6**, 242.
- C. Goh, R. J. Kline, M. D. McGehee, E. N. Kadnikova and J. J. M. Frechet, *Appl. Phys. Lett.*, 2005, **86**, 122110.
- V. C. Sundar, *et al.*, *Science*, 2004, **303**, 1644.
- C. He, Q. G. He, X. D. Yang, G. L. Wu, C. H. Yang, F. L. Bai, Z. G. Shuai, L. X. Wang and Y. F. Li, *J. Phys. Chem. C*, 2007, **111**, 8661.
- L. L. Xue, J. T. He, X. Gu, Z. F. Yang, B. Xu and W. J. Tian, *J. Phys. Chem. C*, 2009, **113**, 12911.
- C. He, Q. G. He, Y. P. Yi, G. L. Wu, C. Yang, F. L. Bai, Z. G. Shuai and Y. F. Li, *J. Mater. Chem.*, 2008, **18**, 4085.
- N. M. Kroneneberg, M. Deppish, F. Wurthner, H. W. A. Ledemann, K. Deing and K. Meerholz, *Chem. Commun.*, 2008, 6489.
- T. Rousseau, A. Cravino, T. Bura, G. Ulrich, R. Ziessel and J. Roncali, *Chem. Commun.*, 2009, 1673.
- L. Valentini, D. Bagnis, A. Marrocchi, M. Seri, A. Taticchi and J. M. Kenny, *Chem. Mater.*, 2008, **20**, 32.
- F. Silvestri, M. D. Irwin, L. Beverina, A. Facchetti, G. A. Pagani and T. J. Marks, *J. Am. Chem. Soc.*, 2008, **130**, 17640.
- A. B. Tamayo, B. Walker and T. Q. Nguyen, *J. Phys. Chem. C*, 2008, **112**, 11545.
- A. B. Tamayo, X. D. Dang, B. Walker, J. Seo, T. Kent and T. Q. Nguyen, *Appl. Phys. Lett.*, 2009, **94**, 103301.
- B. Walker, A. B. Tamayo, X. D. Dang, P. Zalar, J. H. Seo, A. Garcia, M. Tantiwivat and T. Q. Nguyen, *Adv. Funct. Mater.*, 2009, **19**, 1.
- J. Roncali, P. Leriche and A. Cravino, *Adv. Mater.*, 2007, **19**, 2045.
- Y. W. Li, L. L. Xue, H. Li, Z. F. Li, B. Xu, S. P. Wen and W. J. Tian, *Macromolecules*, 2009, **42**, 4491.
- M. Svensson, F. L. Zhang, S. C. Veenstra, W. J. H. Verhees, J. C. Hummelen, J. M. Kroon, O. Inganäs and M. R. Andersson, *Adv. Mater.*, 2003, **15**, 988.
- G. L. Wu, G. J. Zhao, C. He, J. Zhang, Q. G. He, X. M. Chen and Y. F. Li, *Sol. Energy Mater. Sol. Cells*, 2009, **93**, 108.
- K. P. Li, J. L. Qu, B. Xu, Y. H. Zhou, L. J. Liu, P. Peng and W. J. Tian, *New J. Chem.*, 2009, **33**, 2120.
- Y. Yang, J. Zhang, Y. Zhou, G. G. Zhao, C. He, Y. F. Li, M. Andersson, O. Inganäs and F. L. Zhang, *J. Phys. Chem. C*, 2010, **114**, 3701.
- Y. Shirota and H. Kageyama, *Chem. Rev.*, 2007, **107**, 953.
- Y. Shirota, *J. Mater. Chem.*, 2005, **15**, 75.
- Y. Shirota, *J. Mater. Chem.*, 2000, **10**, 1.
- B. C. Thompson, Y. G. Kim and J. R. Reynolds, *Macromolecules*, 2005, **38**, 5359.
- M. M. Alam and S. A. Jenekhe, *Chem. Mater.*, 2002, **14**, 4775.
- L. L. Woods, *J. Am. Chem. Soc.*, 1958, **80**, 1440.
- M. H. Sun, J. Li, B. S. Li, Y. Q. Fu and Z. S. Bo, *Macromolecules*, 2005, **38**, 2651.
- P. F. Xia, X. J. Feng, J. P. Lu, S. W. Tsang, R. Movileanu, Y. Tao and M. S. Wong, *Adv. Mater.*, 2008, **9999**, 1.
- Y. W. Li, L. L. Xue, H. J. Xia, B. Xu, S. P. Wen and W. J. Tian, *J. Polym. Sci., Part A: Polym. Chem.*, 2008, **46**, 3970.
- D. M. D. Leeuw, M. M. J. Simenon, A. R. Brown and R. E. F. Einerhand, *Synth. Met.*, 1997, **87**, 53.
- B. Thompson, Y. Kim and J. Reynolds, *Macromolecules*, 2005, **38**, 5359.
- J. A. Mikroyannidis, S. S. Sharma, Y. K. Vijay and G. D. Sharma, *ACS Appl. Mater. Interfaces*, 2010, **2**, 270.
- Y. Y. Liang, D. Q. Feng, Y. Wu, S.-T. Tsai, G. Li, C. Ray and L. P. Yu, *J. Am. Chem. Soc.*, 2009, **131**, 7792.
- Z. F. Li, J. N. Pei, Y. W. Li, B. Xu, M. Deng, Z. Y. Liu, H. Li, H. G. Lu, Q. Li and W. J. Tian, *J. Phys. Chem. C*, 2010, **114**, 18270.
- P. W. M. Blom, M. J. M. deJong and M. G. vanMunster, *Phys. Rev. B: Condens. Matter*, 1997, **55**, 656.